Monopile as Part of Aeroelastic Wind Turbine Simulation Code

Rune Rubak and Jørgen Thirstrup Petersen
Siemens Wind Power A/S
Borupvej 16
DK-7330 Brande
Denmark

Abstract

The influence on wind turbine design loads of variations in stiffness and damping of a monopile foundation with soil interaction is demonstrated through a case study, which takes non-linearities into account. The study illustrates the importance of a detailed foundation model, and demonstrates the framework, which is an important part of a successful optimization of wind turbines. In particular for offshore wind turbines at deep water sites the optimization and a thorough modelling of the foundation become increasingly important due to the increasing relative cost of the foundation. The main design requirements are – apart from requirements to strength of the foundation itself – related to the limitation of maximum deflection at the tower base and to the stiffness, which influences the vibration modes of the complete structure and particularly the frequencies of the fundamental, transversal tower modes. In order to limit dynamic amplification of the rotor loads, which contain components that are multiples of the rotor rotational frequency, there must be a safe separation of structural and excitation frequencies.

The loads are calculated by use of a fully non-linear aeroelastic wind turbine simulation code, BHawC, which operates in the time domain. The code is developed at Siemens Wind Power during the recent four years. The model discretization is based on finite elements, and the monopile is composed of a series of beam elements. The interaction with the soil is modelled by distributed, non-linear springs and dampers. The external loads include aerodynamic loads and wave loads. The case study is kept within realistic limits by using an existing 2.3 MW wind turbine with a monopile foundation at the Samsø offshore site as the base design.

1. Introduction

Due to cost considerations, the flexibility of the support structure for offshore wind turbines tends to be an important factor for determination of design loads, when the offshore sites are at relatively deeper waters. Often, the monopile foundation is an attractive choice at these sites, and it is chosen in a case study to demonstrate how the structural properties of the foundation and its interaction with the soil influence the dynamic behaviour of the wind turbine structure and the resulting design loads. The study is based on time domain simulations with a fully non-linear aeroelastic code, which is presented initially. It is assumed that the soil consists of sand with uniform properties, which are varied in a parametric study. Due to the non-linear behaviour of the soil pressure as function of deformation, it is important that the code is capable of representing non-linearities, especially when the extreme load range is approached.

2. Aeroelastic code

The presented simulation results are obtained by a new generation aeroelastic code, BHawC (**B**onus Energy **H**orizontal **a**xis **w**ind turbine **C**ode), developed at Bonus Energy A/S and Siemens Wind Power A/S during the recent four years. The main aim with this development is to ensure detailed representation of geometrical non-linearities for all design critical components. The code represents the structure by a geometrically non-linear finite element model, and the aerodynamic load calculation is based on the BEM method with extensions aiming at taking dynamic flow behaviour into account.

2.1 Level of code verification

During the recent year BHawC has gradually taken over the main part of the aeroelastic analysis work at Siemens Wind Power A/S from the HawC code developed at Risø. However, the HawC code is still used for special types of analysis and for verification purposes. Comparison of simulation results from the two codes has been an important part of the verification task, both with respect to direct validation of results but also with respect to transfer of analysis experience to the new generation code. An example of an important validation case study is the detailed comparison of design loads obtained by the two codes for a 2.3 MW stall regulated wind turbine. Despite the different model capabilities of the two codes, the simulated design loads show convincing overall agreement within 5.0%, and for many components even within 1.5%.

Furthermore, simulation results from BHawC have been compared successfully with full scale measurements on the 2.3 MW Mk-II turbine and the 3.6 MW turbine at the Høvsøre test site. The load verification process is ongoing and tends to be more detailed and directed towards specific components in parallel with extension and further development of the code.

2.2 Structural model

The modelling principle, which is used in the BHawC code and which makes it a fully geometrically non-linear model, is usually denoted the principle of co-rotating elements. The deformation of each element is described in a local co-rotating coordinate system, which follows the rigid body movement of the element. The location and the orientation of the co-rotating frame are described with respect to a global reference coordinate system, within which the equations of motion are formulated and solved. In the local frame of reference many parallels can be drawn to linear FEM theory in order to check the implementation.

The main structural parts are modelled by use of a 2 node co-rotational Timoshenko beam element. The beam element supports modelling of different positions of the centre of gravity, the centre of shear, and the elastic axis. In addition a number of specialized elements are used for the different bearings and the gearbox. The structural components, which are represented in the wind turbine model can be identified in the schematic drawing in Figure 1 with further details in Figure 2–Figure 5. The specific model of the monopile foundation for the present case study is shown in Figure 6, and details about the soil spring model are presented in Section 4. With respect to structural details the main difference between BHawC and HawC is in the nacelle and in the drive-train, these components being far more detailed in BHawC.

The nacelle has separate support elements for the main bearings, which on the other hand supports the main shaft exactly where the true main bearings are located. Further, there is an element towards the rear end, which may be used for attachment of drive train support components as shown in the figure, where the generator and the brake caliper supports are attached to the rear node of this element and the gear support is attached to the front node. The rear nacelle element is also a structural member, which typically can be used to attach concentrated mass and mass moment of inertia representing non load-carrying parts, so that the total mass and inertia of the nacelle can be adjusted to the correct values and the resulting location of the centre of gravity can be obtained.

The gearbox is modelled with a low-speed shaft and a high-speed shaft. The high-speed shaft with the brake disk and the generator rotor rotates with the true speed.

The yaw-bearing and the pitch-bearing elements permit elastic deformations about one axis. These elements may be assigned a stiffness, which represents the stiffness of the elements that connect the fixed and the rotating parts of the bearings, i.e. the yaw-gear shaft connection and the pitch cylinder connections. In this way these bearings are realistic parts of the dynamic model.

The solution of the equations of motion is based on an incremental method, which updates the geometry and the kinematics incrementally as the structure deforms. There is no limitation on the capability to represent deformed geometry, as long as the single beam elements do not deform more than the linear element formulation allows. The model has passed one of the basic test cases for large deformation models, where a blade with uniform cross section is loaded with a torque on the tip until it deforms to a circular shape, i.e. the blade tip reaches the blade root.

The model formulation offers the possibility to solve the complex eigenvalue problem, which supplies the damped mode-shapes, the damped natural frequencies and the logarithmic decrement. This also works for a turbine with the drive-train and the rotor free to rotate, i.e. for the non-braked turbine, and the free drivetrain mode-shapes and natural frequencies can be found directly.

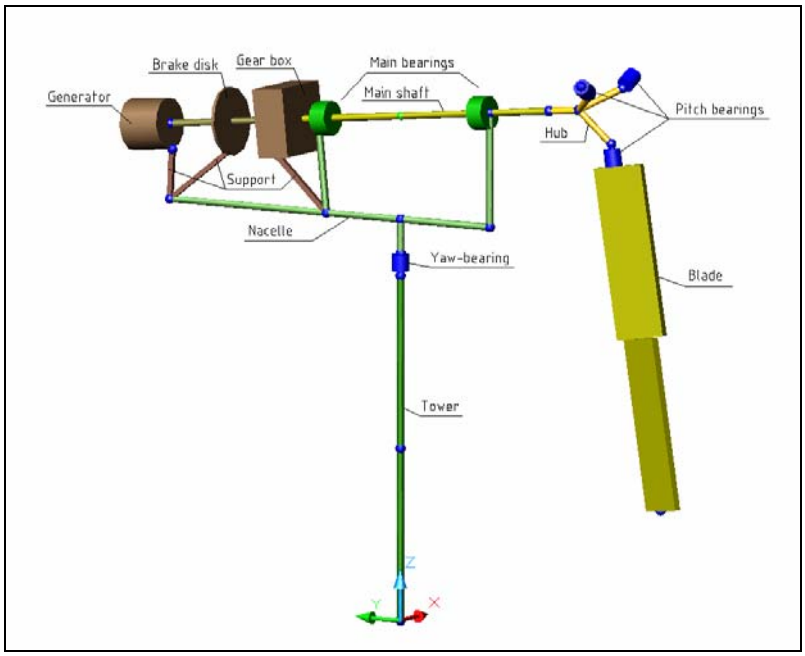

Figure 1: Substructures and components of the BHawC model.

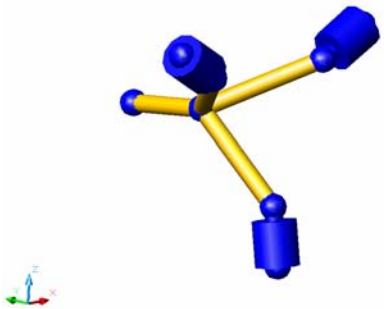

Figure 2: Hub with pitch bearings.

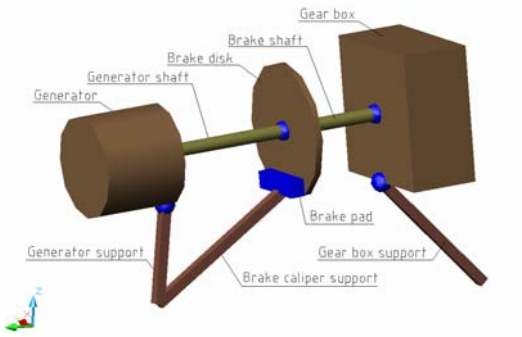

Figure 3: Drive-train components.

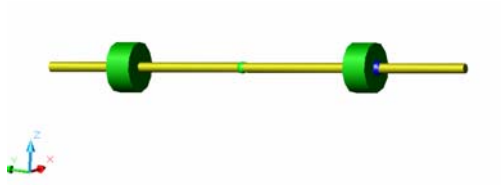

Figure 4: Main shaft with bearings. The actual shaft is modelled by use of 4 elements. Any number of elements may be used.

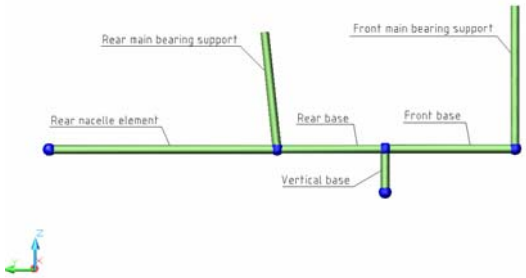

Figure 5: Nacelle elements.

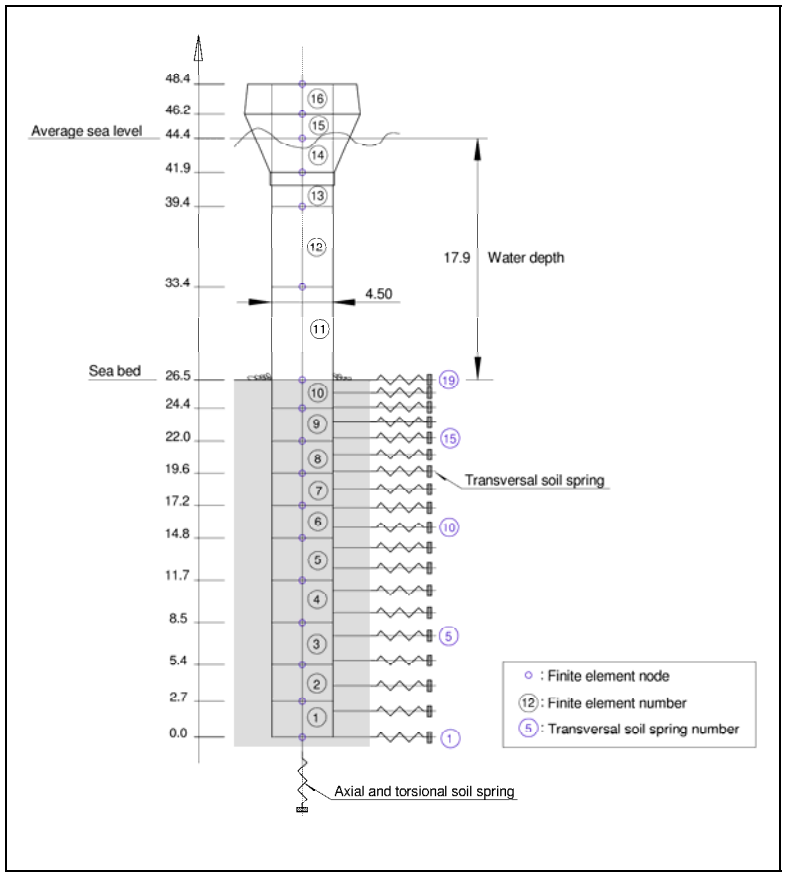

Figure 6: Structural BHawC model of the monopile consisting of 16 beam elements. The lateral interaction with the soil is modelled by distributed, non-linear springs, which may represent the local soil conditions in two perpendicular, horizontal directions. A single spring determines the boundary conditions at the monopile tip with respect to vertical deformation and torsional deformation about a vertical axis. The shown spring distribution corresponds to the target distribution, which is subject to adjustment, when the soil section covered by a spring is confined to the actual extension of the structural finite elements. The actual modification results in totally 27 springs.

2.3 External loads

The external loads may be included as

- Gravity loads.
- Aerodynamic loads on blades, nacelle, tower and free part of the foundation.
- Wave loads on foundation.

The aerodynamic load calculation model is basically the BEM (blade element momentum) model, but with modifications accounting for the influence of dynamic flow effects and the influence of yawed wake. The atmospheric boundary layer turbulence is included as a 3-dimensional, 3-component field with resolution matching the requirements to representation of the frequency content and the spatial structure of the turbulence.

The wave load is time varying and included either as a representative, concentrated load or as a load distributed along the foundation.

In general, all distributed loads are transformed to the finite element nodes consistent with the principle of virtual work.

3. Wind turbine base design

The base design of the wind turbine used in the case study below is almost identical with one of the 2.3 MW stall regulated wind turbines installed at the Samsø offshore site. The rotor diameter is 82.4 m and the hub height is 61.1 m relative to average sea level. The rotational frequency of the rotor at nominal power is 0.277 Hz (1P). The water depth is 17.9 m with respect to average sea level. The soil depth and the dimensions of the foundation are as indicated in Figure 6.

4. Details of soil spring model

The interaction between the monopile and the soil is modelled by distributed, non-linear springs and dampers. The spring distribution is governed by specification of linearly varying separation as function of soil depth. The soil spring model is primarily based on the theory and the recommendations in [1] and [2]. Variations of soil type and soil parameters with soil depth, as specified in the input data, may be accounted for by appropriate choice of spring separation. The distributed spring loads are transformed to the finite element nodes consistent with the principle of virtual work, and the tangential stiffness is calculated according to the actual deformation.

The target distribution of soil springs in the present case study is indicated in Figure 6. The model can handle different soil types, but in the study the soil is arbitrarily assumed to be sand with uniform properties. For sand the lateral soil force per unit vertical length is expressed by the function

$$p(\varphi, D, \gamma', z_s, x) = Ap_u \tanh(\frac{kz_s}{Ap_u} x)$$

where

φ is the friction angle,
D is the monopile diameter,
γ' is the submerged unit weight of the soil,
z_s is the soil depth,
x is the lateral deformation of the soil,
A is a factor depending on the load conditions, either static or cyclic,
$p_u = \min(p_{us}, p_{ud})$ with
$p_{us} = (C_1 z_s + C_2 D)\gamma' z_s$,
$p_{ud} = C_3 D \gamma' z_s$, where
$[C_1, C_2, C_3] = [C_1(\varphi), C_2(\varphi), C_3(\varphi)]$ are functions of the friction angle, and
$k = k(\varphi)$ is a function of the friction angle.

The time varying soil stiffness at 15 m/s wind speed is shown in Figure 7 as function of soil depth. Due to uniform soil properties, the curves approach a straight line, when the deformations approach zero. The slope of the straight line

reflects the soil density. Note that the target distribution of the soil springs has been modified according to the actual element limits, so the total number of springs has changed from the target of 19 springs to the actual 27 springs.

The non-linear behaviour of the soil is indicated in Figure 8, which shows the soil force corresponding to the single springs, normalized with ultimate strength, as function of deformation. The slope of the un-normalized curves determines the soil stiffness.

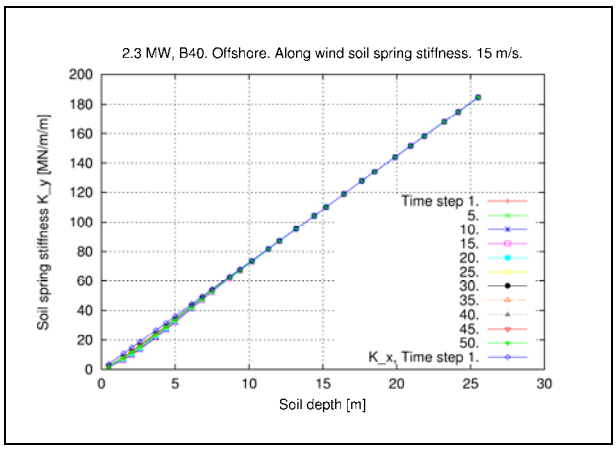

Figure 7: Stiffness in along wind direction as function of soil depth with time step as parameter. The soil is assumed to be uniform sand. Each data point represents a spring.

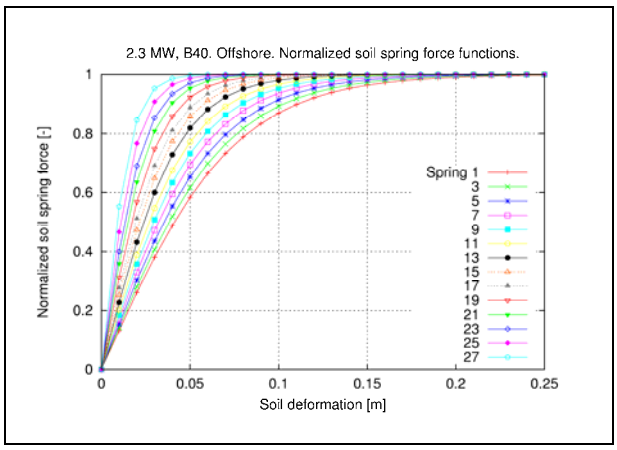

Figure 8: Soil force normalized with ultimate strength as function of deformation with soil depth as parameter. The slope of the un-normalized curves determines the soil stiffness. The soil is assumed to be uniform sand.

5. Deformation and loads during operation

To demonstrate the performance of the monopile model, a time simulation has been performed. The wind speed is 15 m/s and the turbine is exposed to wave load. In Figure 9–Figure 12 snapshots are shown of the transversal soil deformations and forces as function of soil depth at selected simulation time steps. The time step increment is 0.02 sec. meaning that the temporal separation between consecutive curves in the figures is 0.1 sec., and the curves represent a time period of 1 sec. The curves intersect – approximately – at soil depth 17.0 m, indicating that the pile rotates about this point, which is also the position in the pile with maximum cross sectional shear force.

In Figure 13 and Figure 14 the corresponding cross sectional forces and moments at the monopile finite element nodes are shown as function of time.

Figure 15 and Figure 16 show snapshots of cross sectional shear force and moment, respectively, obtained by integration of the distributed soil spring forces. The snapshots correspond to time 1 sec. in Figure 13 and Figure 14, and good agreement can be observed. The non-zero shear force at the monopile tip is explained by the finite separation between the soil springs.

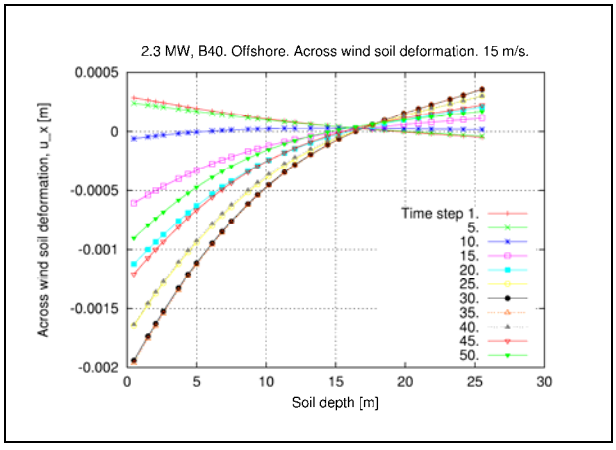

Figure 9: Across wind soil deformation during operation at 15 m/s as function of soil depth with simulation time step as parameter.

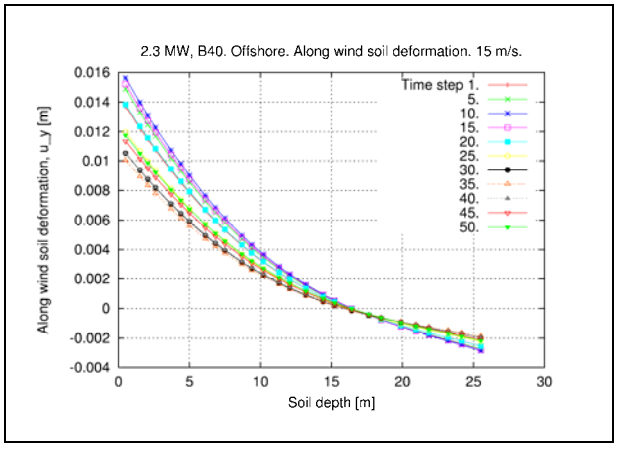

Figure 10: Along wind soil deformation during operation at 15 m/s as function of soil depth with simulation time step as parameter.

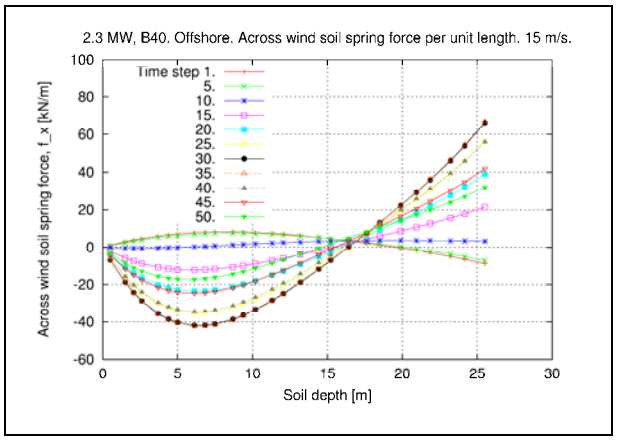

Figure 11: Across wind soil force during operation at 15 m/s as function of soil depth with simulation time step as parameter.

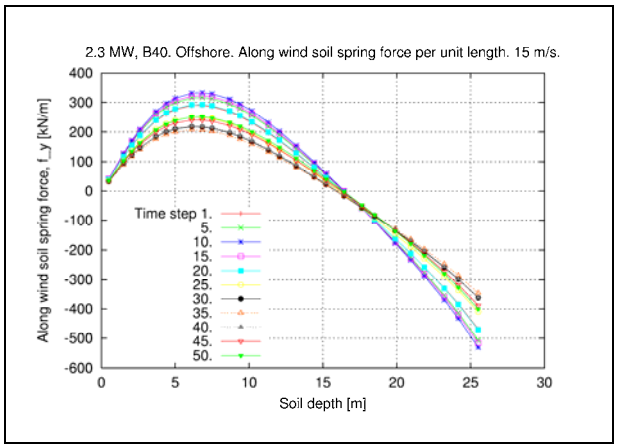

Figure 12: Along wind soil force during operation at 15 m/s as function of soil depth with simulation time step as parameter.

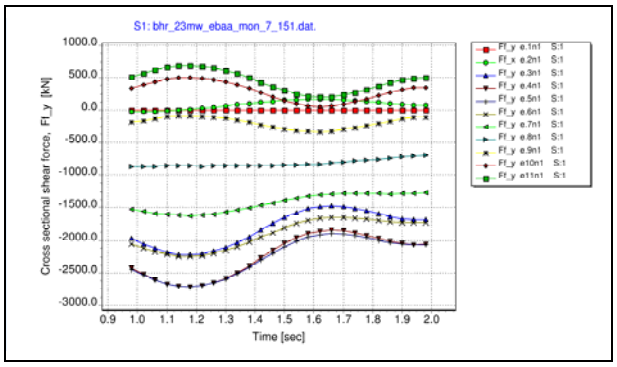

Figure 13: Monopile cross sectional shear force at selected nodes in along wind direction during operation at 15 m/s. The labels in the legend, e.g. e9n1, refer to the beam element number (9) and the local element node number (1, towards the monopile tip).

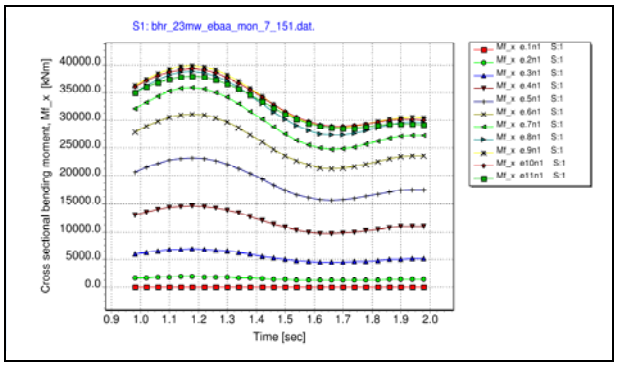

Figure 14: Monopile cross sectional bending moment at selected nodes about an axis in across wind direction during operation at 15 m/s. The labels in the legend, e.g. e9n1, refer to the beam element number (9) and the local element node number (1, towards the monopile tip).

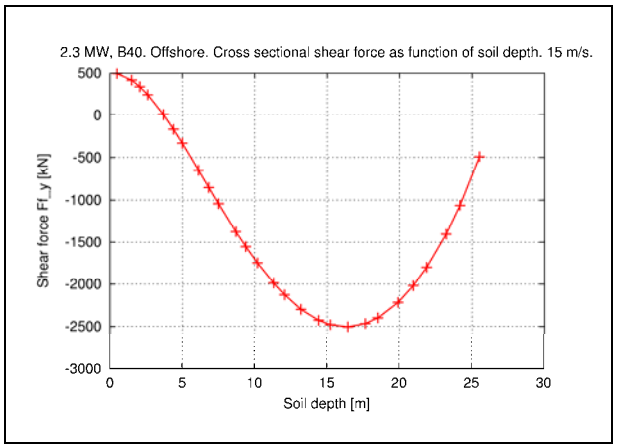

Figure 15: Snapshot of monopile cross sectional shear force in along wind direction during operation at 15 m/s as function of soil depth. The snapshot corresponds to time 1 sec. in Figure 13.

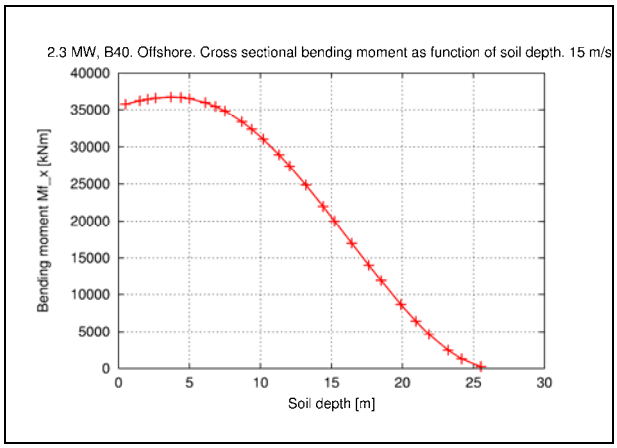

Figure 16: Snapshot of monopile cross sectional bending moment about an axis in across wind direction during operation at 15 m/s as function of soil depth. The snapshot corresponds to time 1 sec. in Figure 14.

6. Influence of uniform variation of soil strength

The importance of modelling the interaction between the monopile and the soil is investigated in a case study, where the strength properties of the sand is varied uniformly along the pile by varying the friction angle:

Calculation case 1: Friction angle $\varphi_1 = 30°$,

Calculation case 2: Friction angle $\varphi_2 = 24°$ and

Calculation case 3: Friction angle $\varphi_3 = 36°$.

6.1 Natural frequencies

The corresponding natural frequencies for the braked turbine in the undeformed state are listed and plotted in Figure 17. Significant change of frequencies takes place only for the fundamental transversal tower modes (-4.0%,+6.0%) and the 2nd rotor tilt and rotor yaw modes (-7.0%,+13.0%).

Generally, a decrease of the fundamental, transversal tower mode frequencies will increase excitation from 1P (0.277 Hz) and from the wave load, which has peak-frequency just below 1P for most wind speeds. The change of the 2nd rotor tilt and yaw frequencies might influence the aerodynamic damping of the edgewise blade mode shapes and change the conditions for stall induced edgewise vibrations. This is confirmed by the simulations in the present study, which show that the edgewise blade vibration increases as the 2nd rotor mode frequencies approach the blade edgewise frequency. These two sets of requirements to the frequencies influenced by the resulting foundation stiffness are contradicting and shows that a full aeroelastic analysis is important.

Natural frequencies						
Sequential number	Natural mode description	Frequency [Hz] Calculation case			Change relative to case 1 [%] Calculation case	
		1	2	3	2	3
1	Tower across wind	0.378	0.365	0.399	-3.5	5.5
2	Tower along wind	0.382	0.368	0.404	-3.6	5.8
3	Shaft torsion	0.571	0.569	0.575	-0.4	0.7
4	1. rotor yaw	0.867	0.867	0.867	0.0	0.0
5	1. rotor tilt	0.911	0.908	0.915	-0.3	0.4
6	1. flapwise	0.977	0.975	0.980	-0.2	0.3
7	2. rotor tilt	1.410	1.322	1.588	-6.3	12.7
8	2. rotor yaw	1.420	1.327	1.601	-6.5	12.7
9	1. edgewise (2-0)	1.636	1.634	1.667	-0.1	1.9
10	1. edgewise (2-1)	1.671	1.667	1.710	-0.2	2.4

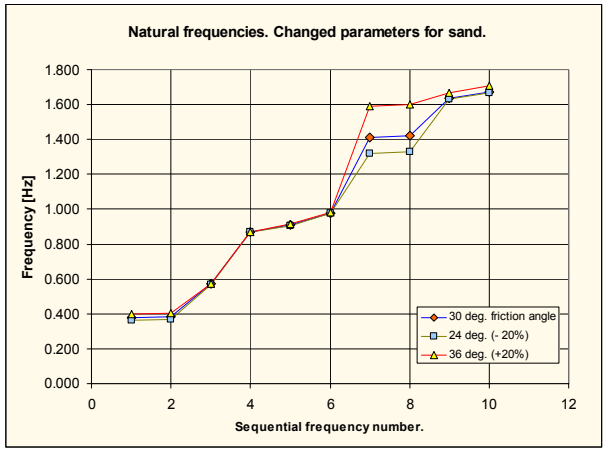

Figure 17: Natural frequencies corresponding to different friction angles for sand.

6.2 Time simulation

Time simulations, each covering a 10 minutes time period, have been performed at wind speeds 10, 15, 20 and 25 m/s for each of the 3 soil conditions defined above.

Standard deviations of the maximum cross sectional shear force and the maximum cross sectional bending moment are shown in Figure 18 and Figure 19, respectively, as function of wind speed. The relatively high standard deviations at 20 m/s are explained by relatively low aerodynamic damping on the rotor in the wind speed range around 20 m/s. Note that the force and the moment are only approximately maximum, as the node positions are not exactly where the maximum is found.

The changes of standard deviation for case 2 ($\varphi_2 = 24°$) and case 3 ($\varphi_3 = 36°$) relative to case 1 ($\varphi_1 = 30°$) are listed in Table 1. It is observed that the change in standard deviation is roughly proportional with the change in fundamental tower frequency, which makes sense, as the excitation frequencies (1P and wave load peak frequency) are fixed, while the transfer function frequency (the fundamental tower frequency) changes.

The cross sectional shear force and bending moment along the soil covered part of the monopile at 25 m/s are shown in Figure 20 and Figure 21, respectively, for the 3 different soil conditions. The soil depth with maximum shear force shifts about 5 m between the extreme soil types, while the corresponding position with maximum bending moment shifts only about 2 m. So, the position with the maximum design moment is rather insensitive to changes in soil.

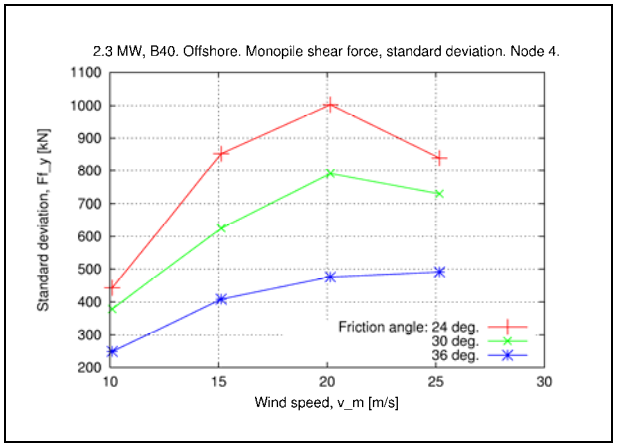

Figure 18: Standard deviation of (approximately) maximum cross sectional shear force.

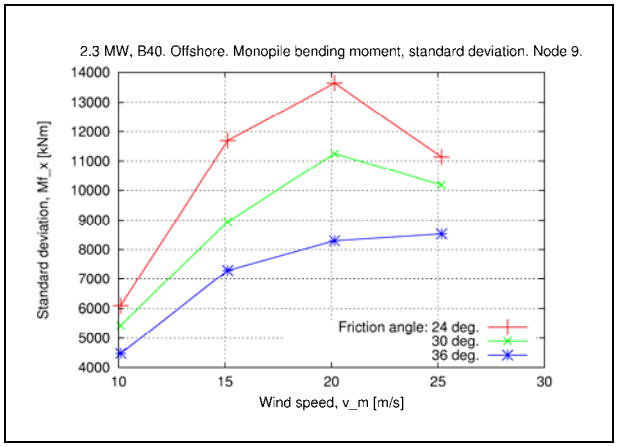

Figure 19: Standard deviation of (approximately) maximum cross sectional bending moment.

Standard deviation of maximum cross sectional bending moment			
Wind speed	Case 1	Change relative to case 1	
		Case 2	Case 3
[m/s]	[kNm]	[%]	[%]
10.1	5432.2	12.2	-17.6
15.1	8939.8	30.8	-18.5
20.1	11248.7	21.3	-26.2
25.2	10180.8	9.4	-16.2

Table 1 Relative change of standard deviation of maximum cross sectional bending moment.

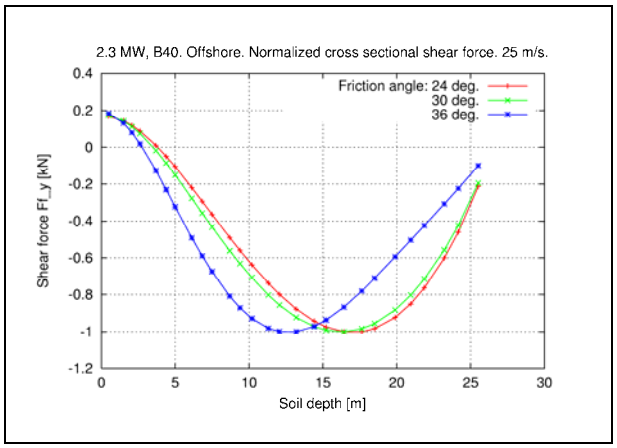

Figure 20: Normalized cross sectional shear force along the monopile at 25 m/s.

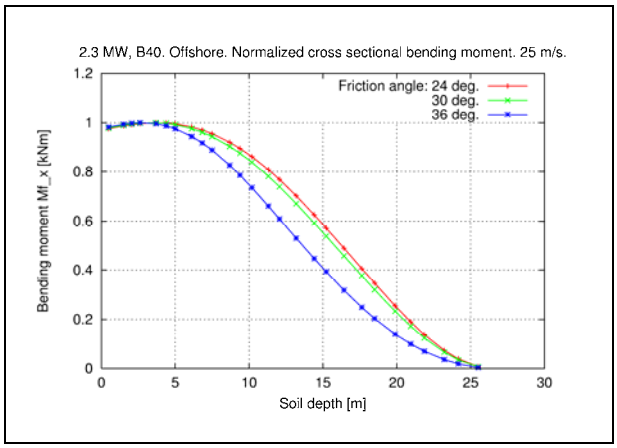

Figure 21: Normalized cross sectional moment along the monopile at 25 m/s.

7. Conclusion

The aeroelastic simulation results in the case study with changing soil conditions show that the model of the monopile as integrated part of the aeroelastic model is rather important, as the dynamic behaviour of the whole wind turbine structure depends strongly on the properties of the foundation. This might influence not only the design loads for the foundation but also design loads for other components. In the present study the vibration level of the edgewise blade mode increases as the soil strength increases.

The study also shows that the position with the maximum cross sectional moment in the monopile is rather insensitive to the soil conditions.

References

[1] G.Kazimierz & M.Jacobsen, *Bearing Capacity and Settlement of Piles*. First edition, Aalborg University, June 1992.

[2] DNV-OS-J101, *Design of Offshore Wind Turbine Structures*. DNV, Denmark, 2004.